Evolution Law and Mechanism of Residual Stress in Ring Components by Cold Ring Rolling Method

Hechuan Song[1,2,*], Xiaomin Zhou[1,2], Qingdong Zhang[1,2] , and Boyang Zhang[1,2]

[1]School of Mechanical Engineering, University of Science and Technology Beijing, Beijing, China
[2]Shunde Innovation School, University of Science and Technology Beijing, Foshan, China
Email: songhechuan@ustb.edu.cn (H.C.S.); zhouxiaomin@ustb.edu.cn (X.M.Z.); Zhang_qd@me.ustb.edu.cn (Q.D.Z.); zhangby@ustb.edu.cn (B.Y.Z.)
*Corresponding author
Manuscript received June 14, 2024; revised July 15, 2024; accepted August 27, 2024; published September 19, 2024.

***Abstract*—Quenching treatment is usually used to improve the mechanical properties of the age-strengthening aluminum alloy. However, high residual stress is introduced during the quenching process, which seriously affects the subsequent manufacturing and service performance. Therefore, the elimination and homogenization of residual stress are particularly important. Based on this, a new and effective method, Cold Ring Rolling (CRR) stress relief, was proposed in this paper. Taking the 2219 Al alloy ring widely used in the aerospace field as an example, the evolution and distribution of residual stress during CRR were explored. The potential danger of the test ring deformation before and after CRR was analyzed with the strain energy density theory. Based on the experimental results, the internal mechanism of residual stress relief by CRR was revealed. The results show that the circumferential and axial residual stress relief rates of the test ring after CRR are 32.35% and 37.86%, respectively, and the degree of residual stress non-uniformity is greatly reduced. At the same time, the strain energy density of the test ring greatly reduces after CRR, and the trend of adverse deformation is effectively reduced. The relief of internal stress is achieved through the initial stage of plastic deformation. Meanwhile, the disordered high-energy defects tend towards a newly ordered low-energy equilibrium. This study can provide theoretical and technical support for the shape control of high-performance ring components.**

***Keywords*—aluminum alloys, cold ring rolling, residual stresses, residual strain energy, evolution mechanisms**

I. Introduction

High-performance ring components are key connecting components of launch vehicles and aircraft cabins [1–4]. For the age-strengthening aluminum alloy ring components, they must undergo solution treatment and quenching after rolling to improve the toughness, strength, fatigue resistance, and corrosion resistance of the material [5]. However, after solution quenching, the ring components will generate significant quenching residual stress, causing deformation and even warping in subsequent mechanical processing, seriously affecting the dimensional accuracy of the components [6–9]. It cannot meet the strict requirements of high-precision thin-walled structural components for residual stress control. Therefore, the control of residual stress for high-performance As-Quenched (AQ) ring components is extremely important.

There are many methods for residual stress relief, including mechanical method [10], thermal aging [11], vibration aging [12], and thermal-vibration aging [13]. However, it is not entirely suitable for the ring components, especially for small batch products, which often require significant investment and the results are not satisfactory. Therefore, there is a need for more economical, convenient, and suitable process methods to be widely promoted and applied. Based on this, a Cold Ring Rolling (CRR) stress relief method is proposed. The ring is cold rolled by a ring rolling mill to expand its outer or inner diameter by 1% to 5%, effectively reducing residual stress and processing deformation, and significantly improving the dimensional accuracy of the component. This method does not require the investment of additional equipment and specialized molds, only requires the use of existing ring rolling mills, and has the advantages of low cost and significant effects.

In this paper, the residual stress relief experiment of the 2219 Al alloy AQ ring was carried out by the CRR process, and the evolution and distribution characteristics of residual stress in the process of CRR were studied in depth. At the same time, the change law of residual strain energy density before and after CRR was analyzed. Finally, the internal mechanism of residual stress relief by CRR was revealed based on the experimental results.

II. Materials and Methods

The size of the 2219 Al alloy ring was Φ 490 mm (outer diameter) × Φ 370 mm (inner diameter) × 110 mm (high). The solid solution treatment of 535 ℃ × 120 min was carried out, followed by water quenching, and finally the CRR process was performed to reduce AQ residual stress. In the course of the CRR (Fig. 1(a)), the radial deformation rate of the ring was 4%, the main roll speed was 1 rad/s, the feed speed of the mandrel was 0.1 mm/s, and the axial and guide roll rotated dynamically.

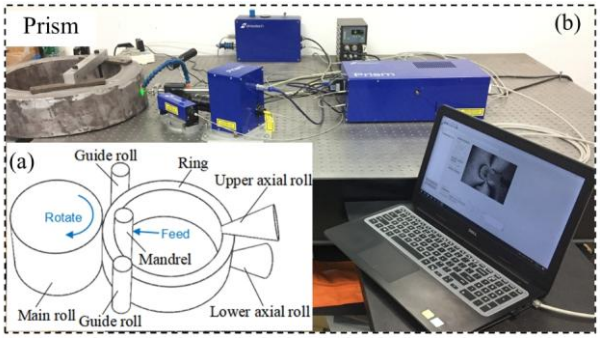

Fig. 1. (a) Schematic diagram of ring cold rolling process and (b)experimental diagram of residual stress detection using Prism.

Residual stress measurement is carried out using a laser small hole stress analyzer-Prism from Finland, which is an advanced drilling system for obtaining accurate residual

stress values (Fig. 1(b)). This equipment is based on the drilling method to remove materials, and combines digital imaging and Electronic Speckle Pattern Interferometry (ESPI) to determine the surface displacement and calculate the pressure. Compared with the standard drilling method, Prism does not need to stick a strain gauge. The operation is simpler, more data points are collected, and the calculation results are more reliable. It can quickly and accurately measure residual stress with a resolution of 7 MPa, suitable for measuring various plane stress states.

During the laser small hole method stress measurement experiment, a hard-alloy micro milling cutter with a diameter of 3.175 mm was used, with a cutting speed of 5000 r/min and measurement depths of 0.2, 0.4, 0.6, 0.8, 1.0, 1.2, 1.4, and 1.6 mm at each point, respectively. The measuring point was located at 1/2 of the wall height on the outer surface of the ring.

At the same time, the X-ray scattering technique was used as an auxiliary measurement method for comparison. The equipment was the Xstress 3000 X-ray diffraction stress meter from AST Finland, and the testing condition was CoKα target material, tube current was 9 mA, a voltage was 30 kV, 2219 aluminum alloy (311) diffraction crystal plane was selected, diffraction angle was 149 °, the exposure time was 20 s, spot size was Φ 3 mm, and the stress of the calibrated stress-free powder was −2.0 MPa.

III. Result and Discussion

A. Residual Stress Amplitude

The residual stress changes in the AQ ring before and after CRR using Prism are shown in Table 1. For a more intuitive analysis, the comparison curve of residual stresses along the depth direction between the AQ ring and the CRR ring is displayed in Fig. 2.

Table 1. Comparison of residual stress in the AQ ring before and after CRR using Prism

Category	Depth/mm	0.2	0.4	0.6	0.8	1.0	1.2	1.4	1.6	Average value
CD	AQ	−146	−176	−226	−127	−126	−118	−56.2	−66.2	−130.18
	CRR	−51.1	−61.6	−81.7	−102	−105	−103	−102	−98.1	−88.06
AD	AQ	−162	−175	−203	−80.1	−38.7	−47.3	7.58	1.4	−87.14
	CRR	−55.2	−72	−90.9	−70.2	−47.3	−35.1	−33.5	−29	−54.15
SD	AQ	−3.56	25.6	20.4	−9.33	−9.67	−0.22	−8.81	−0.72	+1.71
	CRR	−10.6	−9.32	−13.1	−15.8	−15.1	−7.05	−2.46	−0.44	−9.23
Max	AQ	−145	−150	−191	−78.4	−37.6	−47.3	8.77	1.41	−79.89
	CRR	−42.4	−56.1	−72.4	−63.6	−43.6	−34.4	−33.4	−29	−46.86
Min	AQ	−163	−201	−238	−129	−127	−118	−57.4	−66.2	−137.45
	CRR	−63.9	−77.5	−100	−108	−109	−104	−102	−98.1	−95.31

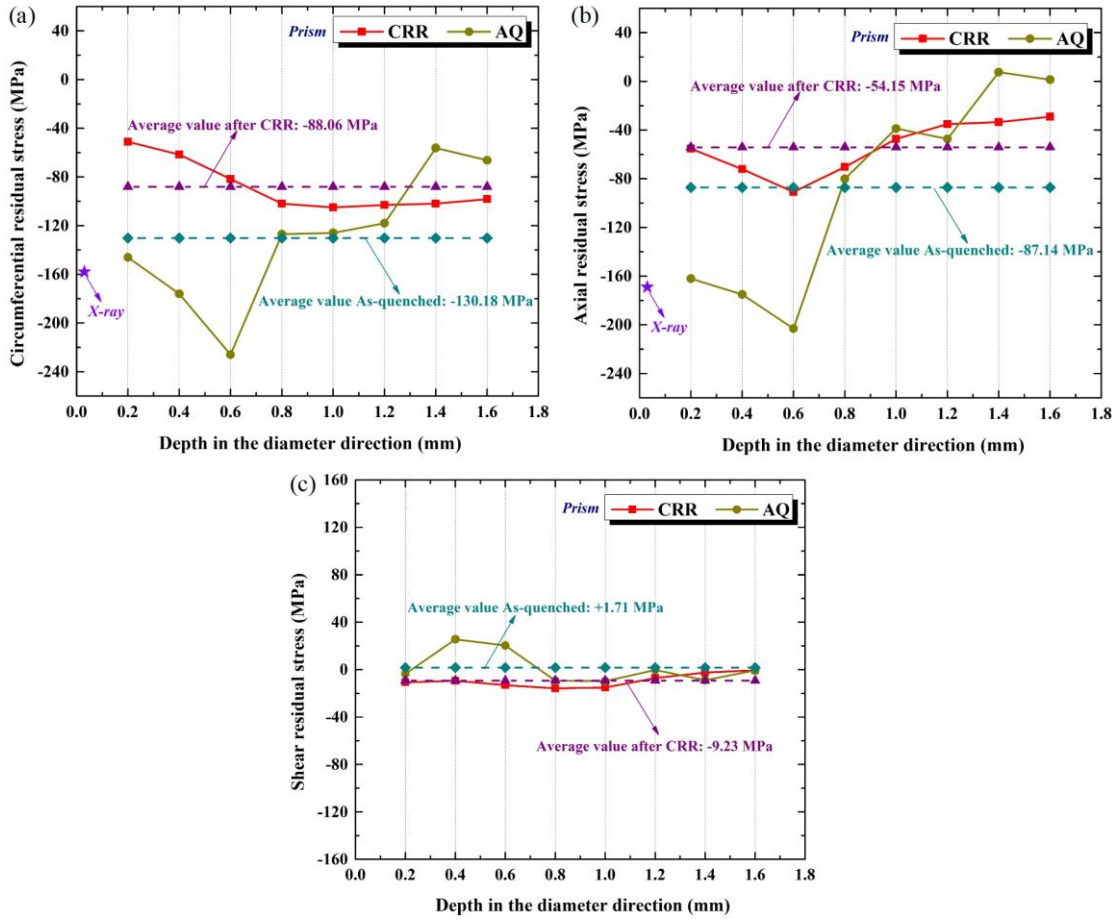

Fig. 2. Comparison of normal/shear residual stress distribution along the depth between the AQ ring and the CRR ring.

It is clear from Fig. 2 that compared to normal residual stresses (Fig. 2(a) and (b)), the shear residual stress is almost small (Fig. 2(c)). The residual stress values of the Prism and X-ray detection methods are consistent, verifying the effectiveness and accuracy of the measurement results (Fig. 2(a) and (b)). Residual stress value roughly shows a trend of first decreasing and then increasing. The residual stresses of the AQ ring are very large and fluctuate violently due to a large temperature gradient caused by the extremely uneven temperature. Compared with the value of the AQ ring, the value of circumferential residual stresses after CRR decreased from −130.18 to −88.06 MPa, with a rate of 32.35% (Fig. 2(a)); the value of axial residual stresses after CRR decreased from −87.14 to −54.15 MPa, with a rate of 37.86% (Fig. 2(b)); the value of shear residual stresses after CRR change from a positive value to a negative value, but the overall change is not significant (Fig. 2(c)). Further compared with the value of the AQ ring, the value of maximum principal stresses after CRR decreased from −79.89 to −46.86 MPa, with a rate of 41.34% (Fig. 3(a)); the value of minimum principal stresses after CRR decreased from −137.45 to −95.31 MPa, with a rate of 30.66% (Fig. 3(b)). The above results indicate that CRR can effectively reduce residual stress amplitude.

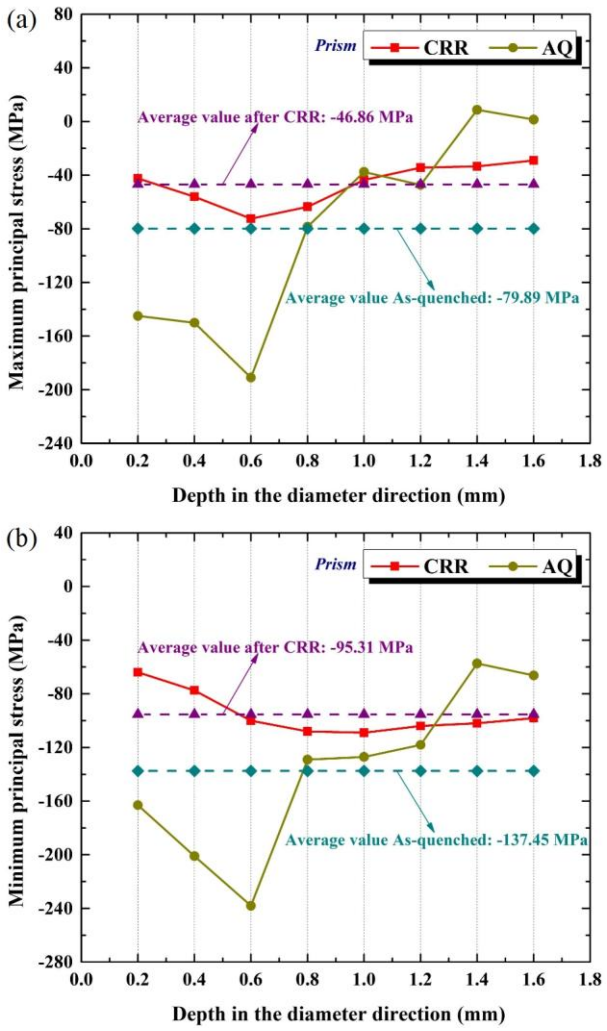

Fig. 3. Comparison of principal residual stress distribution along the depth between the AQ ring and the CRR ring. (a) AQ ring (b) CRR ring.

B. Residual Stress Distribution Uniformity

For a specific form of residual stress distribution, the uniformity of residual stress can be characterized by the range and standard deviation, both of which are positively correlated with the potential dimensional deformation of the component. The calculation formulas for both are:

$$\sigma_R = \sigma_{\max} - \sigma_{\min} \tag{1}$$

$$\sigma_S = \sqrt{\frac{\sum_{i=1}^{n}\left(\sigma_i - \bar{\sigma}\right)^2}{n}} \tag{2}$$

where $\sigma_{\max}$ is the maximum value of residual stress; $\sigma_{\min}$ is the minimum value of residual stress; σ_i is the measurement value of residual stress at each point; $\bar{\sigma}$ is the average value of residual stress; n is the number of measurement points.

Figs. 4 and 5 separately present the ranges and standard deviations of residual stresses before and after CRR. Note, CD, AD and SD represent circumferential, axial and shear residual stress, respectively; Max and Min represent maximum and minimum principal stress, respectively. As is clear from Figs. 4 and 5, compared with the value of the AQ ring, the ranges and standard deviations of residual stresses after CRR decreased in different degrees. The maximum range value decreases from 210.58 to 61.9 MPa, and the reduction rate ranged from 54.34% and 78.27%. The maximum standard deviation value decreases from 73.69 to 20.61 MPa, and the reduction rate ranged from 56.45% and 78.28%. This smaller range and average standard deviation indicate that the residual stress distribution of the CRR ring was more uniform.

C. Residual Strain Energy Density

Elastoplastic deformation inevitably occurs in the manufacturing process of components, and the unreleased elastic strain can be stored in the components in the form of strain energy. At this time, residual stress will be generated in the components. Therefore, the elastic energy stored per unit area of parts in the deformation body, namely the residual strain energy density, can assess the risk of potential deformation of components caused by residual stress. The residual strain energy density can be expressed as:

$$\bar{U} = \frac{1}{2E}\left(\sigma_x^2 + \sigma_y^2 + \sigma_z^2\right) - \frac{\mu}{E}\left(\sigma_x\sigma_y + \sigma_y\sigma_z + \sigma_x\sigma_z\right) + \frac{1}{2G}\left(\tau_{xy}^2 + \tau_{yz}^2 + \tau_{xz}^2\right) \tag{3}$$

where σ_x, σ_y, σ_z represent the normal stress in three directions of X, Y, Z, respectively; $\tau_{xy}, \tau_{yz}, \tau_{xz}$ represent the shear stress on three planes of XY, YZ, XZ, respectively; μ is Poisson's ratio; E is elastic modulus; G is shear modulus.

It can be seen from Fig. 6 that the residual strain energy density within the measured thickness range of the ring before and after CRR decreases from 15897 to 5787, with a decrease of 63.6%. Furthermore, the fluctuation level of residual strain energy density appears noticeably flat. The internal energy of the alloy system tends to be more stable. Meanwhile, it illustrates that the CRR process has an enhancement effect on

the dimensional stability of the ring, thus effectively improving the machining and service accuracy of the components.

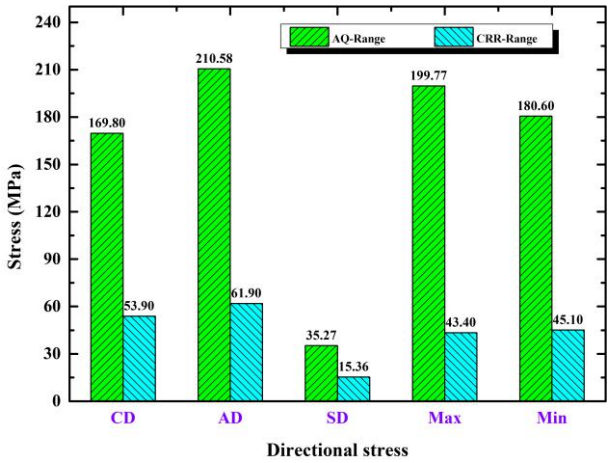

Fig. 4. Ranges of residual stresses of the ring before and after CRR.

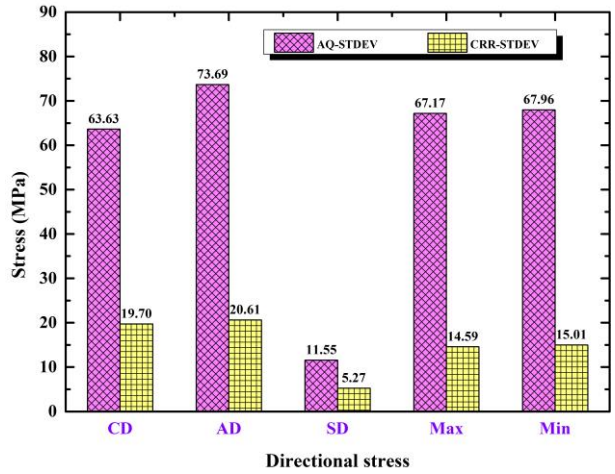

Fig. 5. Standard deviations of residual stresses of the ring before and after CRR.

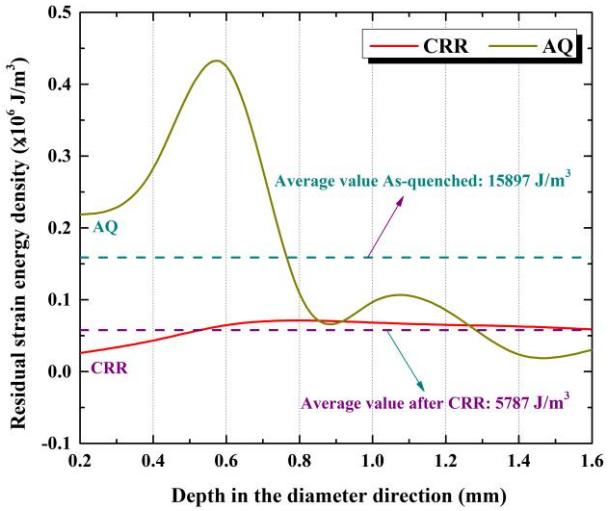

Fig. 6. Change of residual strain energy density before and after CRR.

D. Mechanism of Residual Stress Relief in the CRR Process

The evolution process of the stress field during the CRR process of AQ ring parts is as follows: initial uneven AQ residual stress field→uneven plastic deformation generated by CRR→internal stress field becoming uniform→unloading elastic recovery→residual stress reduction and uniformity.

The macro-micro mechanism of residual stress relief in the CRR process is analyzed as follows.

From a macro perspective, a certain feed rate is applied to the AQ aluminum alloy rings using a ring rolling mill. The relief of internal stress is achieved through the initial stage of plastic deformation. The essence is to redistribute and homogenize the residual stress inside the ring. Furthermore, the purpose of CRR is to generate stress in the ring that is opposite to the AQ residual stress. During this process, the absolute value of residual internal stress and the difference between its positive and negative internal stresses become smaller and smaller (Fig. 7). In theory, as long as the applied plastic deformation is properly controlled, the residual stress amplitude can approach zero.

From a microscopic perspective, when high-strength deformed aluminum alloys are subjected to additional rolling stress fields, the absolute value of the stress sphere tensor increases. At this point, the plastic deformation inside the alloy increases. The disordered high-energy defects in the original alloy begin to move under the action of stress biases, achieving a new ordered low-energy equilibrium. As a result, the density of strain energy inside the alloy decreases, and the residual stress decreases and tends to be more uniform.

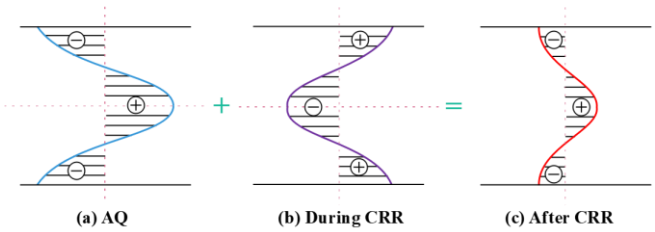

Fig. 7. Schematic diagram of residual stress redistribution in the ring during CRR.

IV. Conclusion

In this paper, the influence law of the CRR method on the magnitude and uniformity of residual stress value and residual strain energy density of the 2219 Al alloy ring were studied. The underlying mechanisms of the effects of CRR on these aspects were then analyzed. Based on the above research, we can draw the following conclusions:

1) The measurement results show that CRR has a desirable effect on relieving and homogenizing residual stress. CRR utilizes existing equipment to relieve residual stress on the ring, which is economical and convenient, providing an effective and practical residual stress control method for rings, especially providing new ideas for residual stress control of large rings.
2) The internal energy of the alloy system tends to be more stable. The trend of adverse deformation is effectively reduced, which shows that the CRR process has an enhancement effect on the dimensional stability of the ring, remarkably improving the service accuracy of the thin-walled structural ring components.
3) The relief of internal stress is achieved through the initial stage of plastic deformation. Correspondingly, the disordered high-energy defects begin to move under the action of stress biases, achieving a newly ordered low-energy equilibrium. As a result, the strain energy density and residual stress inside the alloy greatly reduce and

become more well-distributed.

4) To further improve the efficiency and effectiveness of residual stress relief and homogenization, electromagnetic or heating treatment devices can be added to the basis of CRR. Therefore, electromagnetic-assisted CRR or heating-assisted CRR can be generated, which is also a direction for future development.

CONFLICT OF INTEREST

The authors declare no conflict of interest.

AUTHOR CONTRIBUTIONS

Hechuan Song conducted the data collection, methodology, and writing–original draft preparation; Xiaomin Zhou conducted the conceptualization, writing–review & editing; Qingdong Zhang conducted validation, visualization, and supervision; Boyang Zhang conducted validation, and formal analysis; all authors had approved the final version.

FUNDING

The work is financially supported by the Beijing Natural Science Foundation [Grant No. 3232022]; and the Fundamental Research Funds for the Central Universities [Grant No. FRF-TP-22-035A1]; the authors gratefully acknowledge this support.

ACKNOWLEDGMENT

The authors wish to thank Wuxi Paike New Material Technology Co. Ltd. for providing the experimental components.

REFERENCES

[1] H. L. He, Y. P. Yi, S. Q. Huang, and Y. X. Zhang, "An improved process for grain refinement of large 2219 Al alloy rings and its influence on mechanical properties," *J. Mater. Sci. Tech*., vol. 35, no. 1, pp. 55–63, January 2019.

[2] W. F. Guo, Y. P. Yi, S. Q. Huang, H. L. He and J. Fang, "Effects of warm rolling deformation on the microstructure and ductility of large 2219 Al-Cu alloy rings," *Met. Mater. Int*., vol. 26, pp. 56–68, June 2019.

[3] W. F. Guo, H. L. He, Y. P. Yi, S. Q. Huang, X. C. Mao, J. Fang, and J. W. Huang, "Effects of axial cold-compression on microstructure uniformity and mechanical property enhancement of large 2219 Al-Cu alloy rings," *Mater. Sci. Eng. A*, vol. 798, pp. 140233, November 2020.

[4] Q. Wu, J. Wu, Y. D. Zhang, H. J. Gao, and H. David, "Analysis and homogenization of residual stress in aerospace ring rolling process of 2219 aluminum alloy using thermal stress relief method," *Int. J. Mech. Sci.*, vol. 157–158, pp. 111–118, July 2019.

[5] H. C. Song, H. J. Gao, Q. Wu, and Y. D. Zhang, "Effects of segmented thermal-vibration stress relief process on residual stresses, mechanical properties and microstructures of large 2219 Al alloy rings," *J. Alloy Comp.*, vol. 886, pp. 161269, December 2021.

[6] H. Gong, X. L. Sun, Y. Q. Liu, Y. X. Wu, Y. N. Wang, and Y. J. Sun, "Residual stress relief in 2219 aluminium alloy ring using roll-bending," *Materials*, vol. 13, no. 1, pp. 105, December 2019.

[7] A. Singh and A. Agrawal, "Investigation of surface residual stress distribution in deformation machining process for aluminum alloy," *J. Mater. Process. Tech.*, vol. 225, pp. 195–202, November 2015.

[8] J. D. Cui, Y. P. Yi, and G. Y. Luo, "Numerical and experimental research on cold compression deformation method for reducing quenching residual stress of 7A85 aluminum alloy thick block forging," *Adv. Mater. Sci. Eng.*, vol. 2017, pp. 1–7, Mar 2017.

[9] H. C. Song, Y. D. Zhang, Q. Wu, and H. J. Gao, "Low-stiffness spring element constraint boundary condition method for machining deformation simulation," *J. Mech. Sci. Tech.*, vol. 34, pp. 4117–4128, October 2020.

[10] S. Y. Zhang, Y. X. Wu, and H. Gong, "A modeling of residual stress in stretched aluminum alloy plate," *J. Mater. Process. Tech.*, vol. 212, no. 11, pp. 2463–2473, November 2012.

[11] J. S. Kim, J. H. Yoo, and Y. J. Oh, "A study on residual stress mitigation of the HDPE pipe for various annealing conditions," *J. Mech. Sci. Tech.*, vol. 29, pp. 1065–1073, March 2015.

[12] S. M. Ebrahimi, M. Farahani, and D. Akbari, "The influences of the cyclic force magnitude and frequency on the effectiveness of the vibratory stress relief process on a butt welded connection," *Int. J. Adv. Manuf. Tech*., vol. 102, pp. 2147–2158, January 2019.

[13] H. J. Gao, S. F. Wu, Q. Wu, B. H. Li, and S. Mo, "Experimental and simulation investigation on thermal-vibratory stress relief process for 7075 aluminium alloy," *Mater. Des.*, vol. 195, pp. 108954, October 2020.